







A Coaxial Line Fixture Based on a Hybrid PSO-NLR Model for in Situ Dielectric Permittivity Determination of Carasau Bread Dough

Giacomo Muntoni , *Member, IEEE*, Nicola Curreli , *Member, IEEE*, Davide Toro, Andrea Melis , Matteo Bruno Lodi , *Member, IEEE*, Antonio Loddo, Giuseppe Mazzarella , *Senior Member, IEEE*, and Alessandro Fanti , *Senior Member, IEEE*

Abstract—Food quality is crucial in today’s processing industry. The organoleptic properties of most food materials are known to depend on their water content. The monitoring of food quality and moisture content calls for engineering solutions. To this aim, given their nondestructive nature and cost-effective features, microwave sensors are a valuable tool. However, for some peculiar food processing industries, suitable engineered microwave devices must be designed. Therein, we will focus on the case of the Carasau bread industry. Carasau bread is a typical food product from Sardinia (IT). In this work, we will present the design, realization, and characterization of a coaxial fixture, working between 0.5 and 3 GHz, for the determination of the complex dielectric permittivity of Carasau bread dough. Through a nonlinear regression model based on a particle swarm optimization routine, the scattering parameters are used to retrieve the electromagnetic properties of bread doughs. By making a comparison with the complex dielectric permittivity measured with an open-ended coaxial probe, an average error of 3% for the real part and 6% for the imaginary part has been found. The proposed device is driven by a Raspberry Pi that controls the acquisition of a pocket-vector network analyzer (VNA), thus representing a cost-effective electronic system for industrial applications.

Index Terms—Coaxial fixture, dielectric constant determination, food processing, food properties, nonlinear regression (NLR), particle swarm optimization (PSO).

Manuscript received 18 September 2023; revised 5 February 2024; accepted 23 March 2024. This work was supported in part by the Ministero dello Sviluppo Economico, AGRIFOOD Programma Operativo Nazionale (PON) Imprese e Competitività (I&C) 2014–2020, through the Project “Ingegnerizzazione e Automazione del Processo di Produzione Tradizionale del Pane Carasau Mediante L’utilizzo di Tecnologie IoT (IAPC),” under Grant CUP: B21B19000640008 COR: 1406652 and in part by the Italian Ministry of Enterprises and Made in Italy (MIMIT), “ACCORDI PER L’INNOVAZIONE” (2021–2026), through the Project “Tecnologie ICT e Dell’industria 4.0 per L’analisi e L’ingegnerizzazione di Sistemi Alimentari Complessi per la Produzione di Pani Artigianali Locali ad Alto Valore Aggiunto (AISAC),” under Grant CUP: CUP: B29J23001120005. This article was recommended by Associate Editor C. Josephson. (*Corresponding author: Alessandro Fanti.*)

Giacomo Muntoni, Davide Toro, Andrea Melis, Matteo Bruno Lodi, Giuseppe Mazzarella, and Alessandro Fanti are with the Department of Electrical and Electronic Engineering, University of Cagliari, 09123 Cagliari, Italy (e-mail: gia.como.muntoni@unica.it; davidetoro18@gmail.com; andrea.melis89@unica.it; matteob.lodi@unica.it; mazzarella@unica.it; alessandro.fanti@unica.it).

Nicola Curreli is with the Italian Institute of Technology, 16163 Genoa, Italy (e-mail: nicola.curreli@iit.it).

Antonio Loddo is with the Vecchio Forno SUNALLE, 08023 Fonni, Italy (e-mail: antonio.loddo@sunalle.it).

Digital Object Identifier 10.1109/TAFE.2024.3385185

I. INTRODUCTION

FOOD quality inspection is one of the most discussed topics within the scientific community devoted to the technological development of the agrifood industry. Transition to a digital control, sustainability, traceability, and high quality are the milestones of the path toward the future of the industry [1], [2], [3].

Microwave (MW) devices for the estimation of the dielectric properties of food and food-related products are increasing in popularity for the unmatched advantage of offering accuracy in the measurement process while maintaining a nondestructive approach [4], [5], [6], [7], [8]. The utility is not limited to human food but also to cattle and poultry processed feed [9], [10], covering a large portion of the food processing, and finds application also in adulteration and contamination detection [11], [12], [13], and traceability [14], [15].

The MW measurements of food materials aim to retrieve primarily the moisture content of the product, which is one of the most important indices of the food quality [5], [7], [8]. From an MW engineering point of view, the water presence strongly affects the dielectric signature of the material, thus implying that electromagnetic devices are suitable platforms to characterize food materials. In order to estimate the water content but also the different peculiar characteristics of the food, an MW device’s primary goal is the dielectric characterization of the material through the measurement of the complex permittivity defined as $\varepsilon = \varepsilon' - j\varepsilon''$, wherein ε' is the real part of the dielectric permittivity and ε'' is the imaginary part of the dielectric permittivity, i.e., the so-called loss factor, accounting for the energy losses inside the material, which are proven to be relevant in food products [4]. The dielectric characterization, aimed to retrieve the product moisture, is of significant importance, particularly for baked products, wherein water is one of the main ingredients of the dough. Thus, a reliable and repeatable dielectric estimation of the product is pivotal for both large- and small-scale baked food industries. The latter includes also traditional products, i.e., products that are made following certain technical specifications, or following a traditional recipe, or are regulated by national and/or regional certifications, as in the case of the Carasau bread, a typical Italian flat and crunchy bread made in Sardinia [16]. Carasau bread’s raw ingredients

include remilled semolina of durum wheat, sea salt, natural yeast, and dechlorinated drinking water [3], [17], [18], [19]. The production process of the Carasau is exhaustively explained in [3], [17], [18], and [21], wherein the necessity of having the accurate estimation of the water content inside the dough is highlighted. Briefly, Carasau bread doughs, obtained by kneading the raw ingredients, undergo a first leavening. Then, the doughs are sheeted, go through a second leavening step and finally go through two different baking phases [3], [17], [18], [19], [20], [21]. The dough's water content, therefore, is an information that is pivotal to avoid defected batches due to a suboptimal amount of water. Thus, the accurate dielectric characterization of the Carasau doughs is mandatory to guarantee a waste-free production line. The dielectric characterization of the doughs should be performed *in situ* on several samples of the same batch during the kneading process [17], using a dedicated measurement system. This preventive measurement would allow for an adjustment in the recipe, based on the optimal moisture, by adding more semolina or more water depending on the case. One possible solution is the employment of commercial open-ended coaxial probes (OECs) that are widely used to trace the dielectric profile of solids and liquids [22]. However, commercial coaxial probes are very expensive and they might struggle to work safely within the operating conditions of the bakery, with high temperature and high humidity, as well as the prominent presence of flour dust. Additionally, the measurement process using an OEC demands for a precise calibration protocol. Furthermore, the reliability of the measurement calls for a recalibration after each measurement, or, at least, the assessment of drift effects. All these aspects hamper the adoption of OEC in an industrial scenario [3].

Other approaches can be used to derive the dielectric permittivity of food materials. For instance, inverse scattering procedures, guided-wave approaches, or transmission/reflection (T/R) techniques have been implemented [23], [24], [25], [26], [27], [28], [29], [30], [31], [32], [33], [34], [35], [36], [37], [38], [39], [40], [41], [42], [43]. Even though several devices and methodologies are available, none of them can be immediately applied to the challenging goal of estimating the dielectric permittivity of the Carasau bread doughs during their industrial production.

Given the lack of technological solutions, a low cost, solid, rapid, although accurate alternative, should be employed to empower the small-scale food industry, such as the bakery considered in this work. Preferably, these solutions for industrial applications have to be cost effective. In this framework, they must be interfaced with a miniaturized version of a network analyzer (such as a pocket-vector network analyzer (VNA)) [44]. Pocket-VNA is a performing electronic platform that achieves stable and accurate measurements up to 6 GHz with a very small cost [44]. Furthermore, the use of pocket-VNA would allow to provide protection against the production line's harsh environment, using a suitable case or some sort of coverage, thus ensuring to perform the MW measurements at the production site. In this perspective, it is worth noting that several scientific studies tend to avoid excessively large measurement systems in order to achieve a certain degree of portability, thus making the choice of a pocket-VNA even more appealing [7], [8].

In this work, the electromagnetic device employed for the estimation of the complex permittivity of the Carasau bread dough is a coaxial fixture, made of leaded brass for the metal parts and polylactic acid (PLA) for the sample holder and the alignment gaskets (which are hollow structures). The presented structure has been inspired by the work shown in [38]. In comparison, the coaxial device herein proposed is equipped for solids and liquids dielectric measurements, thanks to the 3-D-printed sample holder that prevents leakage, opening up its employment to a wider range of materials. The device is a part of an *ad hoc* system, connected to a suitable pocket-VNA, whose outputs are read by a Raspberry Pi 4. In order to achieve the accurate dielectric properties of dielectric materials, a hybrid particle swarm optimization (PSO)–nonlinear regression (NLR) model is presented in this work. The algorithm solves, frequency by frequency, the scattering equations with a regression algorithm that finds a perfect match using a nonlinear least-square solution. The absolute minimum was then found using a PSO algorithm.

The hybrid PSO-NLR inversion algorithm is implemented within the board and provides the estimated value of the complex permittivity of the dough in the range of 0.5–3 GHz. The latter frequency range has been chosen considering the entire measurement system, not only the MW device. A low-frequency bandwidth grants good performance, low overall cost of the equipment, and less variability of the complex dielectric permittivity. The estimated values have been compared with the ones obtained, within the same frequency range, using a commercial coaxial probe, showing roughly the same accuracy.

II. LITERATURE REVIEW

Several numerical strategies for the determination of MW dielectric properties are available in the open literature. Most of the work in this area is based on the determination of the scattering parameters, for each frequency in a given range, in order to determine the permittivity parameters, through the explicit or implicit solution of a system of nonlinear scattering equations at each particular frequency [23], [24], [25]. Among guided-wave techniques for the nondestructive determination of the dielectric properties of materials, several open-ended rectangular waveguides [26], [27], [28], [29], rectangular waveguide [30], [31], [32], [33], [34], and coaxial lines' [35], [36], [37], [38], [39] techniques have been developed.

Out of the different techniques, the T/R method is well known for its high accuracy, wide frequency range, and simplicity [38]. For instance, in [39], a method is presented for determining the humidity of granular materials using a two-port MW sensor. From the measurement of the scattering parameters, the complex dielectric constant is derived and, accordingly, the desired properties. The authors in [40] and [41] reported a method to measure the dielectric constant of a liquid material under test based on the measurement of the return loss (S_{11}). In [42], a two-port coaxial sensor is used to calculate the scattering parameters, which were converted to electrical parameters using the Nicolson, Weir, and Ross method, and then a least-square problem is imposed for the extraction of the dielectric constant. A similar method has been

presented in [43] for the extraction of the dielectric constant of the ice.

Considering that past works presenting algorithms for the inverse problem of dielectric permittivity measurements have a variable tradeoff between accuracy and computational time, a different approach for the considered peculiar food industry application has to be sought. In this work, a hybrid solution has been chosen, combining an NLR model that points to an initial guess of the result within the entire operating bandwidth, thus producing an early estimation of the complex dielectric permittivity, with a PSO algorithm that finds the optimal solution using an iterative process. A detailed explanation of the inversion algorithm is reported in Section IV.

III. COAXIAL FIXTURE SENSOR

A. Geometry and Theoretical Foundations

The sensor is modeled as a coaxial fixture with seven different sections, four of which are independent.

- 1) *Sections I and VII*: The initial and final sections of the fixture consist of two standard $50\ \Omega$ coaxial lines employed as an interface between the device and the VNA. The dielectric used in the coaxial cable is Teflon ($\epsilon_r = 2.1$, $\tan\delta = 0.0002$). In the fabricated prototype (see Fig. 4), these sections are represented by the commercial Sub-Miniature version A (SMA) connectors.
- 2) *Sections II and VI*: The conical sections are tapered transmission lines that match the input coaxial line to the central line. These conical sections have a length equal to 54.5 mm. For a perfect alignment of the device and to sustain the structure, four 3.75-mm-thick PLA ($\epsilon_r = 2.54$, $\tan\delta = 0.015$) gaskets, two per conical section, are located in the initial and final part (see Fig. 1).
- 3) *Sections III and V*: They are employed to separate the central section from the conical ones and to effectively create a socket for the sample holder. As in the conical sections, they host two hollow PLA gaskets (one per section) for alignment and support. The length of each section is equal to 30 mm.
- 4) *Section IV*: The central section has a length of 60 mm (bringing the total length of the central section to 120 mm). It hosts the sample holder, a hollow donut-like structure with PLA walls to be fabricated with 3-D printing.

A dimensional drawing of the device is reported in Fig. 1.

The coaxial fixture is entirely enclosed in a metallic shell. The metal chosen for the shell and the inner core is leaded brass, whereas, for the outermost coaxial section, copper has been used.

Each section has been designed to have a $50\ \Omega$ impedance. For the central line and the outermost sections, this condition is easily achievable following the well-known formula [45]:

$$Z = \frac{\zeta}{2\pi\sqrt{\epsilon_r}} \ln \frac{b}{a} \quad (1)$$

wherein ζ is the free-space impedance ($377\ \Omega$), ϵ_r is the permittivity of the dielectric, a is the radius of the core, and b is the radius of the dielectric. For the central line, we have $a = 10\ \text{mm}$ and $b = 25\ \text{mm}$. The most critical sections are

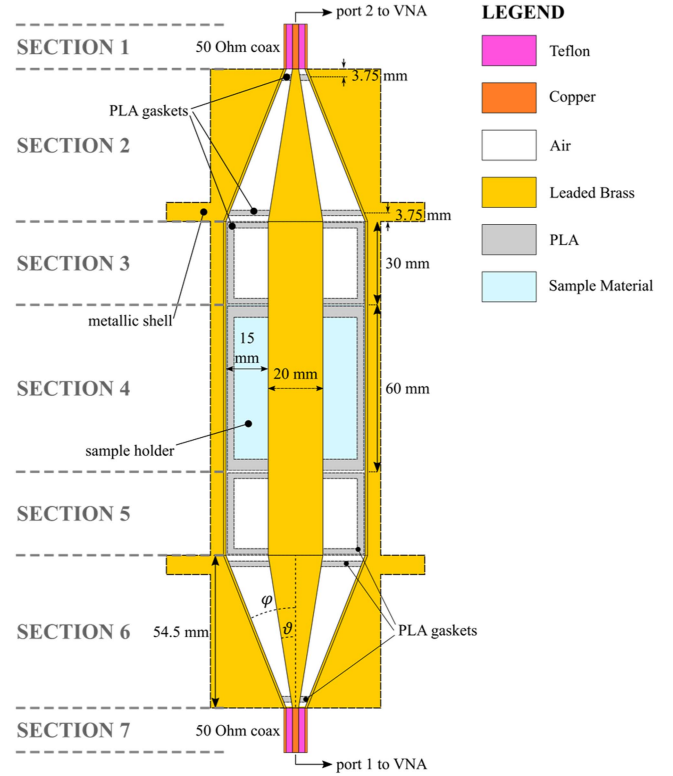


Fig. 1. Dimensional drawing of the coaxial fixture, highlighting the sections and the materials.

the conical ones. In fact, due to the presence of different modes of propagation, the conical section could have different mode impedances, especially at high frequencies. For low frequencies, the fundamental mode impedance formula is defined as follows [46]:

$$Z = \frac{\zeta}{2\pi\sqrt{\epsilon_r}} \ln \frac{\cot(\vartheta/2)}{\cot(\varphi/2)} \quad (2)$$

wherein ϑ is the angle between the coaxial central axis and the inner conductor perimeter and φ is the angle between the coaxial central axis and the outer dielectric perimeter (see Fig. 1 for reference). The first one is given by the difference in diameter between the inner conductor of the central line and the inner conductor of the external line, and by the length of the conical section. Given these values, we have $\vartheta = 0.1745\ \text{rad} = 10^\circ$. The second one is given by the following formula:

$$\begin{aligned} \varphi &= 2 \tan^{-1} \left(2\pi e^{(Z_{\text{conc}}/\zeta)2/\pi} \tan \left(\vartheta/2 \right) \right) \\ &= 0.3973\ \text{rad} = 22.8^\circ. \end{aligned} \quad (3)$$

B. Numerical Study

Once the theoretical foundation has been established, and a presizing of the system has been done, the coaxial fixture has been numerically designed within the CST Studio Suite 2019 (3-Ds, Simulia, DE) simulation environment. In Fig. 2, the scattering parameters of the empty coaxial fixture are shown, displaying a fairly good matching and reasonable losses throughout the entire operating bandwidth (0.5–3 GHz).

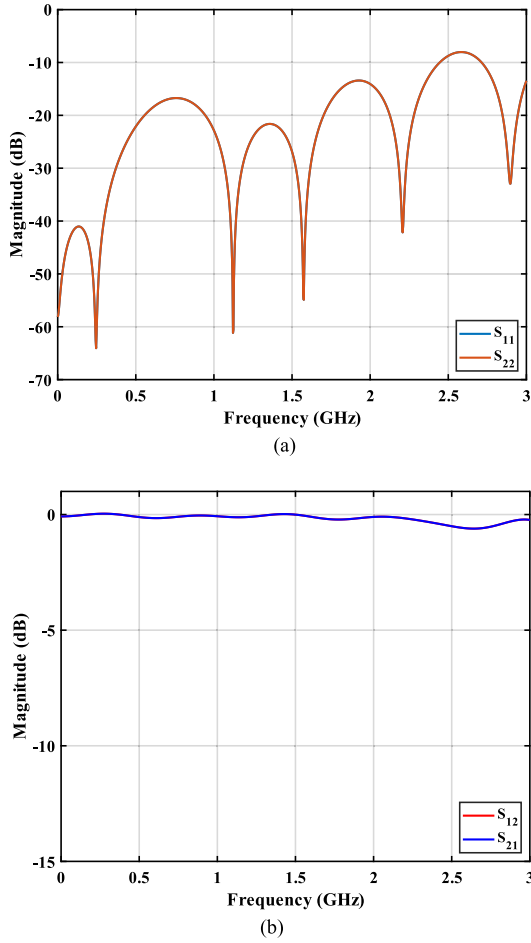


Fig. 2. Simulated scattering parameters of the empty coaxial fixture. (a) Reflection parameters (S_{11} , S_{22}). (b) Transmission parameters (S_{12} , S_{21}).

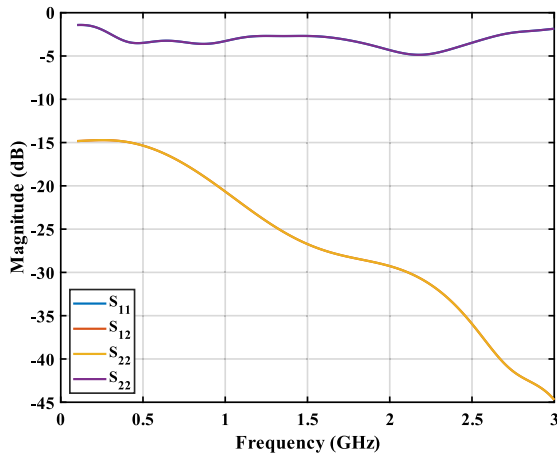
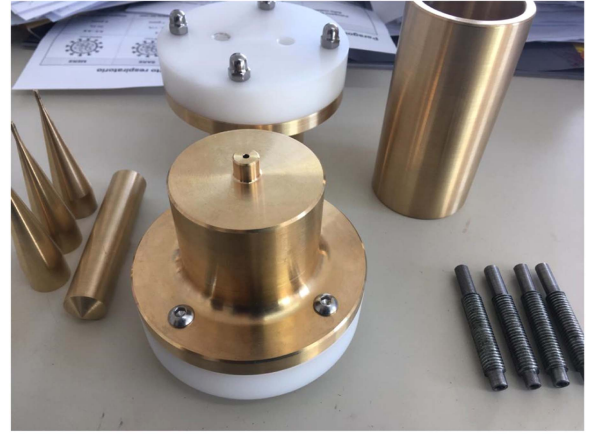
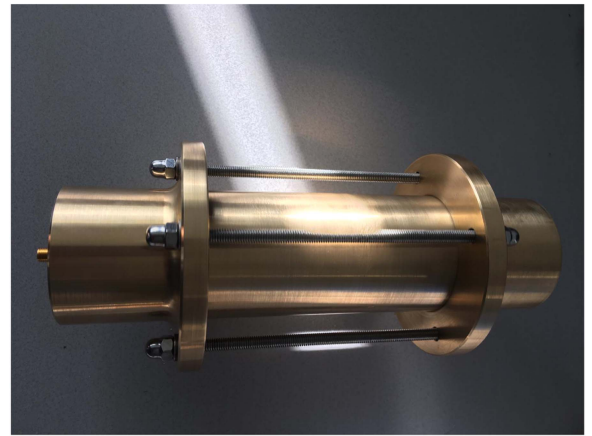


Fig. 3. Simulated scattering parameters of the coaxial fixture with a sample of Carasau bread dough.

Given that the coaxial fixture is supposed to provide information about the complex dielectric permittivity of the Carasau bread dough, we performed numerical simulations to assess in silico how the scattering parameters of the structure would behave when the medium inside the sample holder is the bread



(a)



(b)

Fig. 4. Photos of the realized device. (a) Unassembled coaxial fixture. (b) Assembled coaxial fixture.

dough obtained following the original Carasau recipe (see raw ingredients and dielectric profile shown in [19]).

In Fig. 3, such simulation results are shown. From a direct comparison with Fig. 2, the difference in the frequency response can be observed. The presence of the bread sample is highlighted by the poor impedance matching and the high losses w.r.t. the empty fixture case. From these features of the scattering parameters, it is possible to derive, through a suitable methodology, the dielectric permittivity of the food sample under test placed in Section IV of the device, as shown in Fig. 1.

C. Realization

The coaxial fixture has been realized by the company IFI s.r.l. located in Cagliari (Sardinia), Italy. Photos of the realized prototype are reported in Fig. 4. The metallic components are made of leaded brass (CuZn39Pb2). Since the entire coaxial fixture employs air as a dielectric (with the exception of the external lines where Teflon is used), in order to support the structure integrity, several hollow PLA gaskets are scattered along the body of the coaxial fixture. Their presence can be neglected from an electromagnetic point of view. Other than supporting the structure, these gaskets allow a perfect alignment, which

is essential for the subminiature version a (SMA) connectors soldering.

The coaxial device is enclosed in a cylindrical case, made of leaded brass, and sealed using four long screws and nuts (see Fig. 4). The core of the central section is divided into three parts with conical interlocking. It allows for a fairly convenient insertion of the donut-like sample holder.

It is worth noting that the fabricated prototype has the sole purpose of demonstrating the capability of the presented measurement system. In order to perform the measurement, the fixture has to be disassembled and reassembled, a procedure that is time-consuming and would not be suitable for a commercial scenario. A possible solution could be to separate the coaxial fixture into two main parts, with a threading on the metallic shell, and attach the two main parts to rotating automated arms. This would allow to screw/unscrew the entire coaxial fixture in a matter of seconds. In this case, the dielectric gaskets should be permanently attached to the body of the coaxial fixture, whereas the inner conductor should be divided into two parts, each one permanently connected to a main part of the coaxial fixture, keeping the conical interlocking as in the prototype described in this article. The main concern in this case would be to guarantee the electrical contact of the metallic parts. The sample holder would be the only extractable part of the automated fixture, very much similar to the one described in this article, equipped with a removable lid. This solution would allow a prompt loading/unloading procedure of the coaxial system, suitable for commercial purposes.

IV. INVERSION ALGORITHM

A flux diagram of the inversion algorithm is reported in Fig. 5. After the calibration of the sensor, the first step is the acquisition of the S -parameters using a VNA. The said parameters are then converted into transmission parameters, obtaining the ABCD matrix (i.e., transmission matrix), which is useful to simplify the two-port network. Based on the description of the entire coaxial transmission line provided in Section II, the total transmission matrix can be seen as the product of the transmission matrices of the single sections

$$[T_{\text{tot}}] = [T_{\text{coax}}] * [T_{\text{cone}}] * [T_{\text{air}}] * [T_x] * [T_{\text{air}}] * [T_{\text{cone}}] * [T_{\text{coax}}] \quad (4)$$

wherein T_{coax} is the transmission matrix of the outermost section (a standard coaxial cable with the dielectric component made of Teflon), T_{cone} is the transmission matrix of the conical section, T_{air} is the transmission matrix of the section before the sample, and T_x is the transmission matrix of the section containing the sample. All the transmission matrices are known except for T_x . In order to derive the unknown complex permittivity, a least-square problem has to be solved, in the following form:

$$\begin{aligned} & |A_x(\varepsilon_{\text{Re}}, \varepsilon_{\text{Im}}) - A_{\text{Tot}}|^2 + |B_x(\varepsilon_{\text{Re}}, \varepsilon_{\text{Im}}) - B_{\text{Tot}}|^2 \\ & + |C_x(\varepsilon_{\text{Re}}, \varepsilon_{\text{Im}}) - C_{\text{Tot}}|^2 \text{min!} \end{aligned} \quad (5)$$

wherein A_{Tot} , B_{Tot} , and C_{Tot} are the elements of the total transmission matrix T_{Tot} , whereas A_x , B_x , and C_x are the elements of the unknown transmission matrix T_x . The values ε_{Re} and ε_{Im}

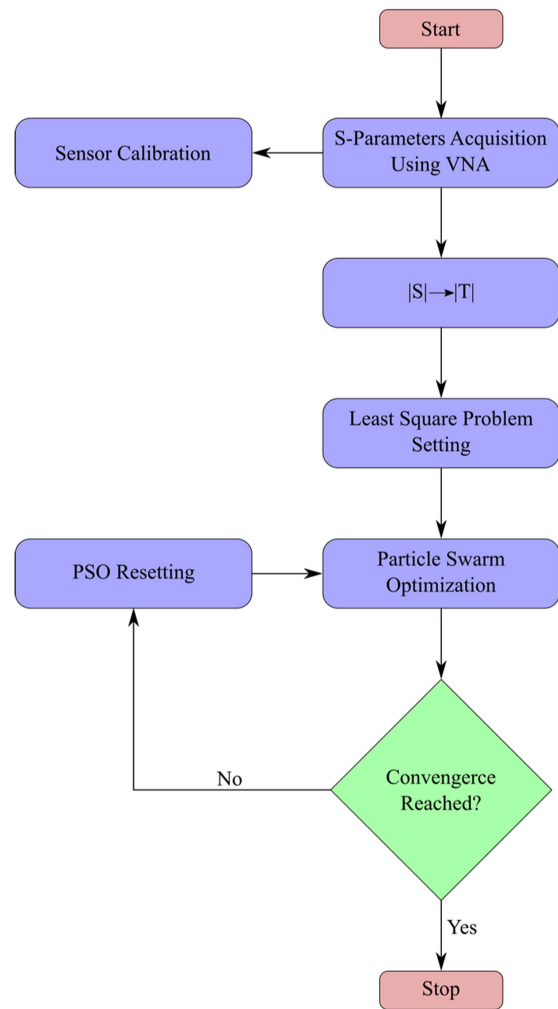


Fig. 5. Flux diagram of the inversion algorithm.

that minimize the function are the real and imaginary parts of the unknown complex permittivity of the sample.

The estimation of the complex permittivity can be intended as a constrained optimization problem in which the global minimum falls inside a given interval [47]. This range of values is relative to a water-based dough, so it is reasonable to fix an interval $\varepsilon' \in [1,100]$ for the real permittivity, and an interval $\varepsilon'' \in [0,100]$ for the imaginary permittivity.

The algorithm has been developed using a MATLAB (v. R2019b, The MathWorks Inc., Cambridge, MA) script, relying on the function *fmincon* and a PSO routine, which is widely used to solve multivariable electromagnetic problems [48]. The employed PSO algorithm is divided into three parts: generation of the particles' position and velocity, updating of the particles' velocity, and updating of the particles' position. These three steps are repeated for every iteration until convergence. The initial position and velocity of the i th particle are randomly determined within the domain at the instant $k = 0$, through the following formulae:

$$x_0^i = x_{\text{min}} + \text{rand}(x_{\text{max}} - x_{\text{min}}) \quad (6)$$

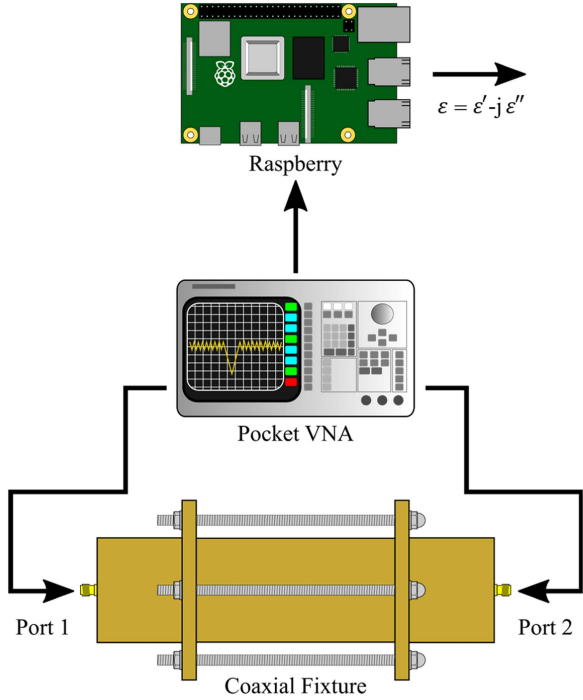


Fig. 6. Schematic representation of the measurement system employed for the experimental validation.

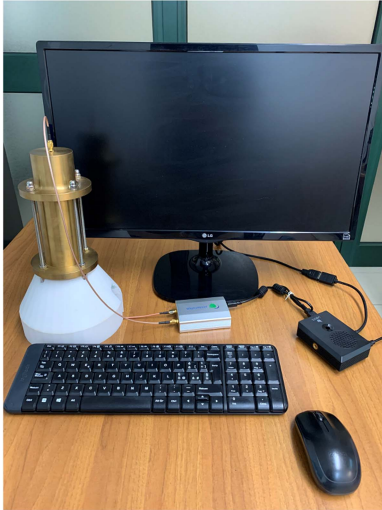


Fig. 7. Measurement system.

$$v_0^i = \frac{x_0^i}{\Delta t} \quad (7)$$

wherein rand is a uniformly distributed random variable. The movement of each particle is influenced by its local best known position and the swarm moves toward the best solution for every given instant. The velocity is updated based on the formula

$$v_{k+1}^i = wv_{k+1}^i + c_1 \text{rand} \frac{(p^i - x_k^i)}{\Delta t} + c_2 \text{rand} \frac{(p_k^g - x_k^i)}{\Delta t}. \quad (8)$$

The first term of this equation indicates the current direction of the particles, the second term represents the influence of the particles' memory, i.e., how much the next direction will be

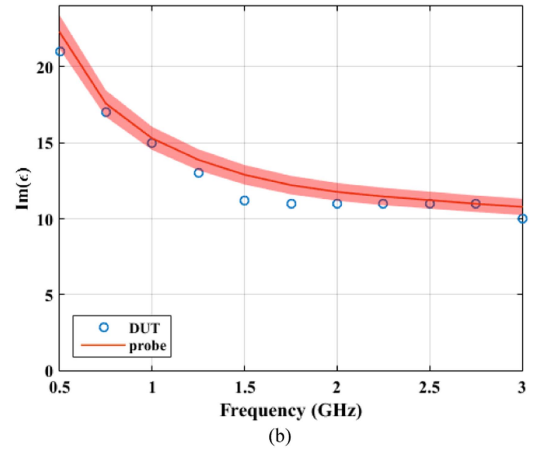
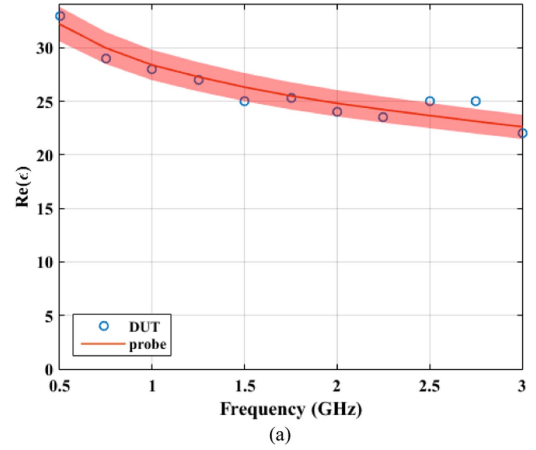


Fig. 8. Comparison between the complex permittivity of the Carasau bread dough with 50% water content measured using the DUT (i.e., the coaxial fixture) depicted as blue circles and using a commercial coaxial probe, depicted as a red line. (a) Real part. (b) Imaginary part.

TABLE I
MEASUREMENT ERROR

	Max Err. (%)	Avg. Err. (%)	RMSE	Std. dev.
Re(ε)	7.50	3.28	0.97	1.01
Im(ε)	15.00	5.95	0.88	0.51

influenced by the previous position of the particle, and the last term represents the influence that the other particles' position has on the i th particle. Finally, the last step is the update of the position at the instant $k + 1$ using the formula

$$x_{k+1}^i = x_k^i + v_{k+1}^i \Delta t. \quad (9)$$

The algorithm stops when one of the following conditions is met.

- 1) The minimum tolerance is reached, i.e., the difference between the minima of one iteration and the previous one is lower than the value imposed as a tolerance.
- 2) The maximum number of iterations is reached, i.e., the algorithm was not able to find the optimum value in a fixed number of iterations.
- 3) The minimum value is found.

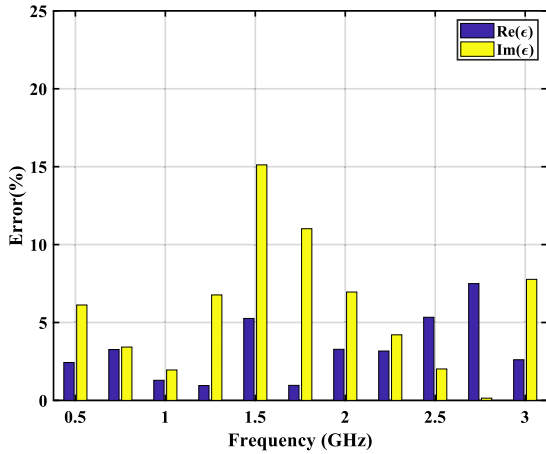


Fig. 9. Percentage error variation of the DUT (coaxial fixture) when compared with the commercial coaxial probe for the real and imaginary part of the complex dielectric permittivity of the original recipe (50% water content) Carasau bread dough.

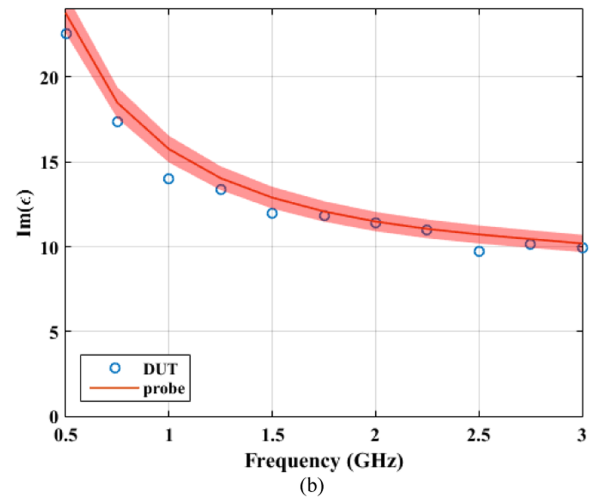
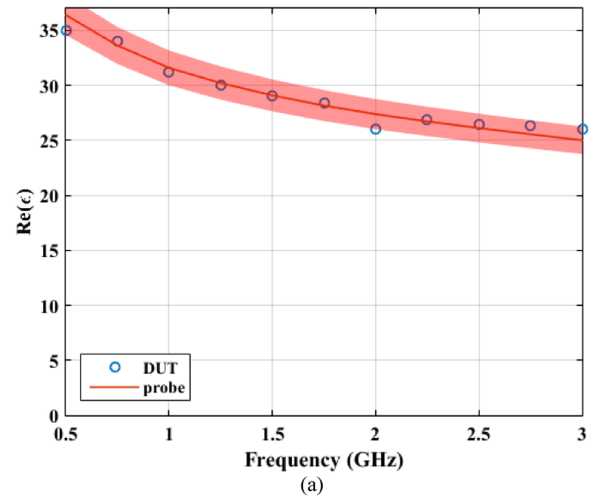


Fig. 11. Comparison between the complex permittivity of the Carasau bread dough with 54% water content measured using the DUT (i.e., the coaxial fixture) depicted as blue circles and using a commercial coaxial probe, depicted as a red line. (a) Real part. (b) Imaginary part.

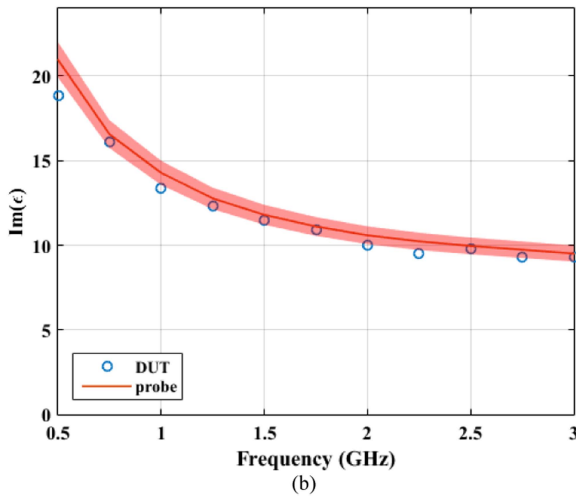
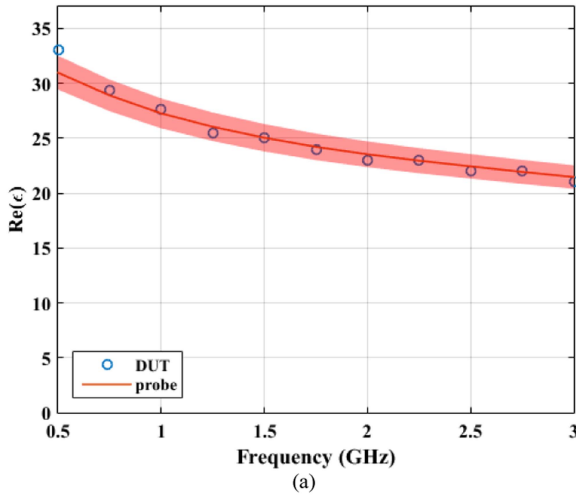


Fig. 10. Comparison between the complex permittivity of the Carasau bread dough with 46% water content measured using the DUT (i.e., the coaxial fixture) depicted as blue circles and using a commercial coaxial probe, depicted as a red line. (a) Real part. (b) Imaginary part.

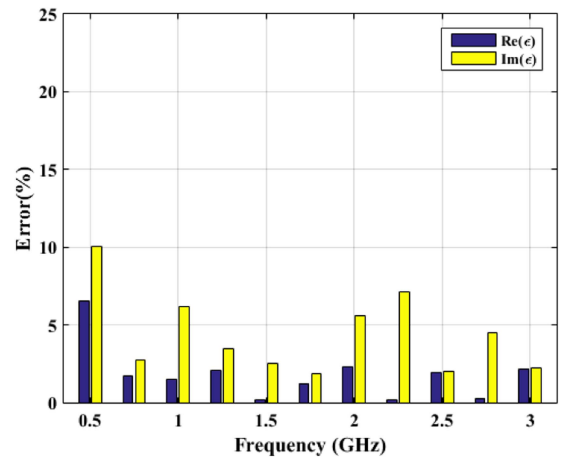


Fig. 12. Percentage error variation of the DUT (coaxial fixture) when compared with the commercial coaxial probe for the real and imaginary part of the complex dielectric permittivity of the Carasau bread dough with 46% of water.

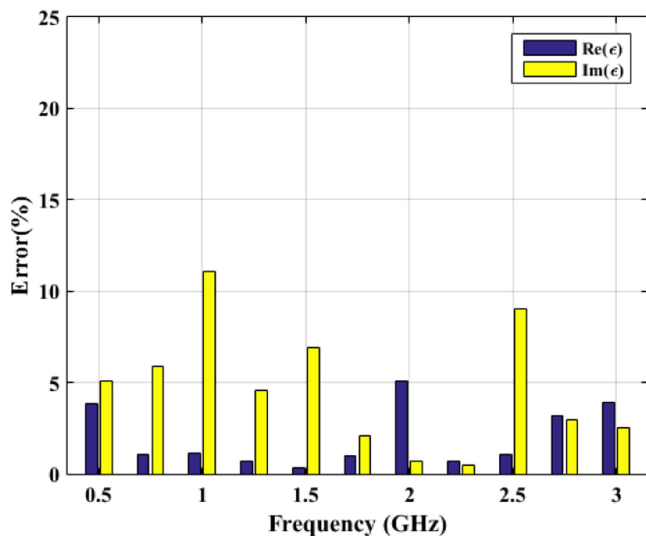


Fig. 13. Percentage error variation of the DUT (coaxial fixture) when compared with the commercial coaxial probe for the real and imaginary part of the complex dielectric permittivity of the Carasau bread dough with 54% of water.

Since the depicted method is statistical, there is no guarantee that the solution found is the optimal value. However, it has been preferred over other heuristic methods (e.g., genetic algorithm) for its ability to operate in large domains and its reduced computational load.

V. EXPERIMENTAL VALIDATION AND RESULTS

The schematic of the electronic measurement system employed for the experimental validation is reported in Fig. 6. The two ports of the coaxial fixture are connected to the pocket-VNA. The output of the VNA (S -parameter matrix) is read by the Raspberry Pi 4. By using the *pocket-VNA Saver* tool, the Raspberry can read the data of the network analyzer from the serial port, extract it, and display it on a monitor. The VNA data can then be saved into a file. Next, the board analyzes such file, runs the algorithm described in Section IV, and provides the complex permittivity of the sample in the operating frequency range. A photograph of the described system is reported in Fig. 7.

For the experimental validation, a dough kneaded with the Carasau bread traditional recipe [3] (50% of water w.r.t. the semolina weight) has been characterized using the coaxial fixture and the resulting complex permittivity has been compared with the one obtained using the commercial DAK 3.5 Speag OECF system [49]. The two samples used for the comparison came from the same batch of Carasau dough. The probe takes ten consecutive measurements of the same sample in a given frequency range. These values are then averaged and they are shown in Fig. 8 as a red line. Considering our previous analyses [3], [19], [21], we also included as a red shaded area the combined standard deviations for the doughs variability and the dielectric probe uncertainties and errors. The comparison is reported in Fig. 8.

From the displayed results, it can be inferred that the coaxial fixture is rather accurate when compared with the output of the commercial measurement system. The information about

the measurement error made using the device under test (DUT) (i.e., the coaxial fixture) w.r.t. the commercial coaxial probe is reported in Table I, whereas Fig. 9 shows the percentage error variation within the operating frequency range. The measurement made with the commercial probe in this case is taken as a reference to calculate the error. The comparison is made every 250 MHz within the frequency range 0.5–3 GHz. The highest inaccuracy (15%) is found for the imaginary part of the complex dielectric permittivity, as expected, since it is usually the most challenging physical quantity to estimate. Nonetheless, the calculated average error for the real and imaginary parts is in the order of 3% and 6%, respectively.

For the sake of completeness and also to estimate the sensitivity of the proposed methodology, the same measurement comparisons have been performed for doughs with an incorrect amount of water, i.e., 46% and 54% w.r.t. the semolina weight, thus diverging from the original recipe. The results of these measurements are reported in Fig. 10 and Fig. 11, respectively, whereas the percentage error variation of the DUT compared with the commercial coaxial probe is reported in Fig. 12 and Fig. 13, respectively. Once again the highest inaccuracy is found for the imaginary part, in both cases, having 10% for the dough with less water and 11% for the dough with more water. The calculated average error for the real and imaginary parts is in the order of 2% and 4.5% for both cases. Considering these values, it can be safely stated that the presented coaxial fixture, coupled with the PSO-NLR algorithm and the *ad hoc* measurement system, has sufficient accuracy to be considered a viable, more rapid, and low-cost alternative to the commercial coaxial probe for the dielectric characterization of the Carasau bread dough within an industrial environment.

VI. CONCLUSION

Food dielectric characterization using MW devices is a viable, low-cost, and nondestructive way to extrapolate some of the most important features of agricultural products. By combining a suitable coaxial fixture based on the mismatching of a coaxial line section and a hybrid PSO-NLR algorithm, a cost-effective and rather accurate MW device for the dielectric characterization of the Carasau bread dough is presented in this article. The coaxial fixture has been tested with a sample of bread dough kneaded following the Carasau bread traditional recipe. The results show that the presented coaxial device is able to provide the accurate estimation of the complex permittivity of the Carasau bread dough when compared with a commercial coaxial probe, resulting in a cost effective, more rapid, and more suitable alternative. The coaxial sensor works within the operating frequency bandwidth of 0.5–3 GHz, taking advantage of the benefits of the low-frequency spectrum, such as low-cost measurement equipment while retaining good performance. The presence of a 3-D-printed sample holder allows for the dielectric estimation of solid and liquid materials, making the coaxial device an attractive solution also for other industrial applications.

ACKNOWLEDGMENT

The authors would like to thank M. Bauco and L. Lorusso from the Rohde and Schwarz Italia for the VNA freely provided, and

F. Di Napoli from the M.F.M. of Urrai Salvatora and C.S.N.C for providing the semolina wheat and for the useful information about the industrial process.

REFERENCES

- [1] L. Cocco et al., "A blockchain-based traceability system in agri-food SME: Case study of a traditional bakery," *IEEE Access*, vol. 9, pp. 62899–62915, 2021, doi: [10.1109/ACCESS.2021.3074874](https://doi.org/10.1109/ACCESS.2021.3074874).
- [2] F. Gandino, B. Montrucchio, M. Rebaudengo, and E. R. Sanchez, "On improving automation by integrating RFID in the traceability management of the agri-food sector," *IEEE Trans. Ind. Electron.*, vol. 56, no. 7, pp. 2357–2365, Jul. 2009, doi: [10.1109/TIE.2009.2019569](https://doi.org/10.1109/TIE.2009.2019569).
- [3] M. B. Lodi et al., "Microwave characterization and modeling of the carasau bread doughs during leavening," *IEEE Access*, vol. 9, pp. 159833–159847, 2021, doi: [10.1109/ACCESS.2021.3131207](https://doi.org/10.1109/ACCESS.2021.3131207).
- [4] S. O. Nelson and P. G. Bartley, "Measuring frequency- and temperature-dependent permittivities of food materials," *IEEE Trans. Instrum. Meas.*, vol. 51, no. 4, pp. 589–592, Aug. 2002, doi: [10.1109/TIM.2002.802244](https://doi.org/10.1109/TIM.2002.802244).
- [5] T. Limpiti and M. Krairiksh, "In situ moisture content monitoring sensor detecting mutual coupling magnitude between parallel and perpendicular dipole antennas," *IEEE Trans. Instrum. Meas.*, vol. 61, no. 8, pp. 2230–2241, Aug. 2012, doi: [10.1109/TIM.2012.2186656](https://doi.org/10.1109/TIM.2012.2186656).
- [6] T. Tantisoparak, H. Moon, P. Youryon, K. Bunya-athichart, M. Krairiksh, and T. K. Sarkar, "Nondestructive determination of the maturity of the durian fruit in the frequency domain using the change in the natural frequency," *IEEE Trans. Antennas Propag.*, vol. 64, no. 5, pp. 1779–1787, May 2016, doi: [10.1109/TAP.2016.2533660](https://doi.org/10.1109/TAP.2016.2533660).
- [7] N. Javanbakht, G. Xiao, and R. E. Amaya, "A comprehensive review of portable microwave sensors for grains and mineral materials moisture content monitoring," *IEEE Access*, vol. 9, pp. 120176–120184, 2021, doi: [10.1109/ACCESS.2021.3108906](https://doi.org/10.1109/ACCESS.2021.3108906).
- [8] L. Fan et al., "A novel handheld device for intact corn ear moisture content measurement," *IEEE Trans. Instrum. Meas.*, vol. 69, no. 11, pp. 9157–9169, Nov. 2020, doi: [10.1109/TIM.2020.2994603](https://doi.org/10.1109/TIM.2020.2994603).
- [9] B. L. Shrestha, H. C. Wood, L. Tabil, O.-D. Baik, and S. Sokhansanj, "Microwave permittivity-assisted artificial neural networks for determining moisture content of chopped alfalfa forage," *IEEE Instrum. Meas. Mag.*, vol. 20, no. 3, pp. 37–42, Jun. 2017, doi: [10.1109/MIM.2017.7951691](https://doi.org/10.1109/MIM.2017.7951691).
- [10] A. Bekal, B. G. Balsubramaniam, V. Awaghade, and S. Ghute, "Application of microwave moisture sensor for DOC and animal feed," *IEEE Sensors J.*, vol. 20, no. 24, pp. 14809–14816, Dec. 2020, doi: [10.1109/JSEN.2020.3010574](https://doi.org/10.1109/JSEN.2020.3010574).
- [11] S. Karuppuswami, A. Kaur, H. Arangali, and P. P. Chahal, "A hybrid magnetoelastic wireless sensor for detection of food adulteration," *IEEE Sensors J.*, vol. 17, no. 6, pp. 1706–1714, Mar. 2017, doi: [10.1109/JSEN.2017.2656476](https://doi.org/10.1109/JSEN.2017.2656476).
- [12] J. A. Tobon Vasquez et al., "Noninvasive inline food inspection via microwave imaging technology: An application example in the food industry," *IEEE Antennas Propag. Mag.*, vol. 62, no. 5, pp. 18–32, Oct. 2020, doi: [10.1109/MAP.2020.3012898](https://doi.org/10.1109/MAP.2020.3012898).
- [13] M. Ricci, J. A. T. Vasquez, R. Scapatucci, L. Crocco, and F. Vipiana, "Multi-antenna system for in-line food imaging at microwave frequencies," *IEEE Trans. Antennas Propag.*, vol. 70, no. 8, pp. 7094–7105, Aug. 2022, doi: [10.1109/TAP.2022.3177436](https://doi.org/10.1109/TAP.2022.3177436).
- [14] F. Gandino, B. Montrucchio, M. Rebaudengo, and E. R. Sanchez, "On improving automation by integrating RFID in the traceability management of the agri-food sector," *IEEE Trans. Ind. Electron.*, vol. 56, no. 7, pp. 2357–2365, Jul. 2009, doi: [10.1109/TIE.2009.2019569](https://doi.org/10.1109/TIE.2009.2019569).
- [15] I. Cuiñas, R. Newman, M. Trebar, L. Catarinucci, and A. A. Melcon, "RFID-based traceability along the food-production chain [wireless corner]," *IEEE Antennas Propag. Mag.*, vol. 56, no. 2, pp. 196–207, Apr. 2014, doi: [10.1109/MAP.2014.6837090](https://doi.org/10.1109/MAP.2014.6837090).
- [16] F. Paschino, F. Gabella, F. Giubellino, and F. Clemente, "The level of automation of 'carasau' bread production plants," *J. Agricultural Eng.*, vol. 38, pp. 61–64, 2007, doi: [10.4081/jae.2007.2.61](https://doi.org/10.4081/jae.2007.2.61).
- [17] G. Muntoni et al., "Designing a microwave moisture content sensor for carasau bread: A feasibility study," in *Proc. 16th Eur. Conf. Antennas Propag.*, 2022, pp. 1–5, doi: [10.23919/EuCAP53622.2022.9769280](https://doi.org/10.23919/EuCAP53622.2022.9769280).
- [18] K. Mannaro et al., "A robust SVM color-based food segmentation algorithm for the production process of a traditional carasau bread," *IEEE Access*, vol. 10, pp. 15359–15377, 2022, doi: [10.1109/ACCESS.2022.3147206](https://doi.org/10.1109/ACCESS.2022.3147206).
- [19] M. B. Lodi, C. Macciò, N. Curreli, A. Melis, G. Mazzarella, and A. Fanti, "Effects of carasau dough composition on the microwave dielectric spectra up to 20 GHz," *IEEE Trans. Agrifood Electron.*, vol. 1, no. 1, pp. 50–57, Jun. 2023, doi: [10.1109/TAFE.2023.3277790](https://doi.org/10.1109/TAFE.2023.3277790).
- [20] F. Fanari, J. Keller, F. Desogus, M. Grosso, and M. Wilhelm, "Impact of water and flour components in dough investigated through low-field nuclear magnetic resonance," *Chem. Eng. Trans.*, vol. 87, pp. 289–294, 2021.
- [21] C. Macciò et al., "Microwave spectroscopy investigation of carasau bread doughs: Effects of composition up to 8.5 GHz," *Foods*, vol. 12, no. 12, 2023, Art. no. 2396.
- [22] S. Joof et al., "A guideline for complex permittivity retrieval of tissue-mimicking phantoms from open-ended coaxial probe response with deep learning," *IEEE Trans. Microw. Theory Techn.*, vol. 70, no. 11, pp. 5105–5115, Nov. 2022, doi: [10.1109/TMTT.2022.3209701](https://doi.org/10.1109/TMTT.2022.3209701).
- [23] S. Roberts and A. Von Hippel, "A new method for measuring dielectric constant and loss in the range of centimeter waves," *J. Appl. Phys.*, vol. 17, no. 7, pp. 610–616, Jul. 1946, doi: [10.1063/1.1707760](https://doi.org/10.1063/1.1707760).
- [24] J. Baker-Jarvis, E. J. Vanzura, and W. A. Kissick, "Improved technique for determining complex permittivity with the transmission/reflection method," *IEEE Trans. Microw. Theory Techn.*, vol. 38, no. 8, pp. 1096–1103, Aug. 1990, doi: [10.1109/22.57336](https://doi.org/10.1109/22.57336).
- [25] H. E. Bussey, "Measurement of RF properties of materials a survey," *Proc. IEEE*, vol. 55, no. 6, pp. 1046–1053, Jun. 1967, doi: [10.1109/PROC.1967.5719](https://doi.org/10.1109/PROC.1967.5719).
- [26] L. Li, H. Hu, P. Tang, B. Chen, J. Tian, and S. Safavi-Naeini, "A modified open-ended rectangular waveguide based reflection approach for dielectric constant characterization of low-loss slab materials," *IEEE Trans. Antennas Propag.*, vol. 69, no. 11, pp. 8009–8014, Nov. 2021, doi: [10.1109/TAP.2021.3076486](https://doi.org/10.1109/TAP.2021.3076486).
- [27] M. Kempin, M. T. Ghasr, J. T. Case, and R. Zoughi, "Modified waveguide flange for evaluation of stratified composites," *IEEE Trans. Instrum. Meas.*, vol. 63, no. 6, pp. 1524–1534, Jun. 2014, doi: [10.1109/TIM.2013.2291952](https://doi.org/10.1109/TIM.2013.2291952).
- [28] M. T. Ghasr, D. Simms, and R. Zoughi, "Multimodal solution for a waveguide radiating into multilayered structures—Dielectric property and thickness evaluation," *IEEE Trans. Instrum. Meas.*, vol. 58, no. 5, pp. 1505–1513, May 2009, doi: [10.1109/TIM.2008.2009133](https://doi.org/10.1109/TIM.2008.2009133).
- [29] N. N. Qaddoumi, W. M. Saleh, and M. Abou-Khousa, "Innovative near-field microwave nondestructive testing of corroded metallic structures utilizing open-ended rectangular waveguide probes," *IEEE Trans. Instrum. Meas.*, vol. 56, no. 5, pp. 1961–1966, Oct. 2007, doi: [10.1109/TIM.2007.904570](https://doi.org/10.1109/TIM.2007.904570).
- [30] G. Yang, S. Zhou, W. Liang, X. Li, H. Huang, and J. Yang, "Effect of different shapes on the measurement of dielectric constants of low-loss materials with rectangular waveguides at X-band," *IEEE Microw. Wireless Compon. Lett.*, vol. 32, no. 12, pp. 1471–1474, Dec. 2022, doi: [10.1109/LMWC.2022.3177400](https://doi.org/10.1109/LMWC.2022.3177400).
- [31] X. Wang and S. A. Tretyakov, "Fast and robust characterization of lossy dielectric slabs using rectangular waveguides," *IEEE Trans. Microw. Theory Techn.*, vol. 70, no. 4, pp. 2341–2350, Apr. 2022, doi: [10.1109/TMTT.2022.3143827](https://doi.org/10.1109/TMTT.2022.3143827).
- [32] D. A. Connelly et al., "Complex permittivity of gadolinium gallium garnet from 8.2 to 12.4 GHz," *IEEE Magn. Lett.*, vol. 12, Dec. 2021, Art. no. 5504504, doi: [10.1109/LMAG.2021.3132850](https://doi.org/10.1109/LMAG.2021.3132850).
- [33] H. Shwaykani, A. El-Hajj, J. Costantine, and M. Al-Husseini, "A calibration-free method for the dielectric constant calculation of low-loss materials," *IEEE Trans. Instrum. Meas.*, vol. 70, Jul. 2021, Art. no. 6000310, doi: [10.1109/TIM.2020.3011765](https://doi.org/10.1109/TIM.2020.3011765).
- [34] M. Kiani, A. Abdolali, and M. Tayarani, "A novel waveguide approach for electromagnetic characterization of inhomogeneous materials," *IEEE Trans. Microw. Theory Techn.*, vol. 66, no. 10, pp. 4658–4665, Oct. 2018, doi: [10.1109/TMTT.2018.2859316](https://doi.org/10.1109/TMTT.2018.2859316).
- [35] H. Hasar et al., "Permittivity extraction of soil samples using coaxial-line measurements by a simple calibration," *IEEE Trans. Geosci. Remote Sens.*, vol. 61, Jan. 2023, Art. no. 5300108, doi: [10.1109/TGRS.2022.3233912](https://doi.org/10.1109/TGRS.2022.3233912).
- [36] N. Mahjabeen and R. Henderson, "Extracting wideband dielectric properties of stacked packaging substrates using coaxial airlines," *IEEE Trans. Microw. Theory Techn.*, vol. 69, no. 1, pp. 887–895, Jan. 2021, doi: [10.1109/TMTT.2020.3037954](https://doi.org/10.1109/TMTT.2020.3037954).
- [37] F. M. Mbango, J. E. Delfort M'pemba, F. Ndagijimana, and B. M'passi-Mabiala, "Use of two open-terminated coaxial transmission-lines technique to extract the material relative intrinsic parameters," *IEEE Access*, vol. 8, pp. 138682–138689, 2020, doi: [10.1109/ACCESS.2020.3012431](https://doi.org/10.1109/ACCESS.2020.3012431).
- [38] Z. Caijun, J. Quanxing, and J. Shenhui, "Calibration-independent and position-insensitive transmission/reflection method for permittivity measurement with one sample in coaxial line," *IEEE Trans. Electromagn. Compat.*, vol. 53, no. 3, pp. 684–689, Aug. 2011, doi: [10.1109/TEMC.2011.2156416](https://doi.org/10.1109/TEMC.2011.2156416).
- [39] S. Trabelsi, A. W. Kraszewski, and S. O. Nelson, "New calibration technique for microwave moisture sensors," *IEEE Trans. Instrum. Meas.*, vol. 50, no. 4, pp. 877–881, Aug. 2001, doi: [10.1109/19.948292](https://doi.org/10.1109/19.948292).

- [40] S. Seewattanapon and P. Akkaraekthalin, "A broadband complex permittivity probe using stepped coaxial line," *J. Electromagn. Anal. Appl.*, vol. 3, no. 8, pp. 312–318, Jul. 2011, doi: [10.4236/jemaa.2011.38050](https://doi.org/10.4236/jemaa.2011.38050).
- [41] L. Oppl, J. Vrba, and R. Zajicek, "Broadband measurement of complex permittivity using reflection method and coaxial probes," *Radioengineering*, vol. 17, no. 1, pp. 14–19, Apr. 2008.
- [42] K. J. Bois, L. F. Handjojo, A. D. Benally, K. Mubarak, and R. Zoughi, "Dielectric plug-loaded two-port transmission line measurement technique for dielectric property characterization of granular and liquid materials," *IEEE Trans. Instrum. Meas.*, vol. 48, no. 6, pp. 1141–1148, Dec. 1999, doi: [10.1109/19.816128](https://doi.org/10.1109/19.816128).
- [43] P. Bohleber, N. Wagner, and O. Eisen, "Permittivity of ice at radio frequencies: Part I—Coaxial transmission line cell," *Cold Region Sci. Technol.*, vol. 82, pp. 56–67, Oct. 2012, doi: [10.1016/j.coldregions.2012.05.011](https://doi.org/10.1016/j.coldregions.2012.05.011).
- [44] Jan. 2024. [Online]. Available: <https://pocketvna.com/>
- [45] B. C. Wadell, *Transmission Line Design Handbook*. Norwood, MA, USA: Artech House, 1991.
- [46] R. D. Beyers and D. I. L. de Villiers, "Design and analysis of an impedance tapered conical to coaxial transmission line transition," in *Proc. 44th Eur. Microw. Conf.*, 2014, pp. 307–310, doi: [10.1109/EuMC.2014.6986431](https://doi.org/10.1109/EuMC.2014.6986431).
- [47] H.-Y. Tseng, P.-H. Chu, H.-C. Lu, and M.-J. Tsai, "Easy particle swarm optimization for nonlinear constrained optimization problems," *IEEE Access*, vol. 9, pp. 124757–124767, 2021, doi: [10.1109/ACCESS.2021.3110708](https://doi.org/10.1109/ACCESS.2021.3110708).
- [48] J. Robinson and Y. Rahmat-Samii, "Particle swarm optimization in electromagnetics," *IEEE Trans. Antennas Propag.*, vol. 52, no. 2, pp. 397–407, Feb. 2004, doi: [10.1109/TAP.2004.823969](https://doi.org/10.1109/TAP.2004.823969).
- [49] Jan. 2024. [Online]. Available: <https://speag.swiss/products/dak/overview/>



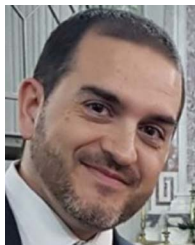
Davide Toro received the bachelor's degree in electronic engineering from the University of Cagliari, Cagliari, Italy, in 2018, and the master's degree in telecommunication engineering from the University of Cagliari, Cagliari, Italy, in 2021.

He was an Assistant Researcher with Electromagnetic Group, University of Cagliari, from 2018 to 2021. Since 2021, he has been a Technical Project Manager with TIM. His research activity involves the design and characterization of microwave components for agrifood applications.



Andrea Melis received the bachelor's degree in biomedical engineering from the University of Cagliari, Cagliari, Italy, in 2017.

He was an Assistant Researcher with the University of Cagliari. His research interests include EM modeling and development of RF coils at low and high frequencies, especially for MRI at high field, the design and realization of WSN systems for the monitoring of industrial processes, such as bread manufacturing, and intelligent transportation systems.



Giacomo Muntoni (Member, IEEE) received the Bachelor's degree in electronic engineering and the Master's degree in telecommunication engineering from the University of Cagliari, Cagliari, Italy, in 2010 and 2015, respectively, and the Ph.D. degree in electronic engineering and computer science from the University of Cagliari, Cagliari, Italy, in 2019.

He is currently working as a Technologist in Applied Electromagnetics Group with the University of Cagliari. His research activity involves the design and characterization of antennas for biomedical and

aerospace applications, microwave-based dielectric characterization of materials, 3-D printing of RF components, and monitoring of the space debris environment in low Earth orbit with Sardinia Radio Telescope, in collaboration with Cagliari Astronomical Observatory.



Nicola Curreli (Member, IEEE) received the M.Sc. degree in biomedical engineering from the University of Genoa, Genoa, Italy, in 2016, and the Ph.D. degree in electronic engineering from the University of Cagliari, Cagliari, Italy, and the Italian Institute of Technology—IIT, Genoa, Italy, in 2020.

After completing the Ph.D. degree, he held a Fellow position with Graphene Labs—IIT, where he contributed to the Graphene Core 2 Project as a part of the Graphene Flagship initiative. In 2019, he was a Visiting Researcher with Physics and Mechanical

Engineering Departments, Columbia University, New York City, NY, USA, as a part of the Marie Skłodowska-Curie RISE Action "SONAR H2020." Between 2022 and 2023, he was a Visiting Researcher with the Molecular Foundry, Lawrence Berkeley National Laboratory, Berkeley, CA, USA. He is currently a Researcher with Functional Nanosystems—IIT, Genova, Italy. His research interests include the study of low-dimensional materials, their characterization, and their application in the field of photonics, and the design, implementation, and analysis of linear and nonlinear integrated optical, microwave devices, and antennas.

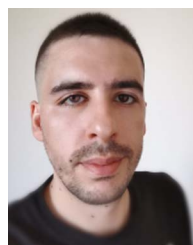
Dr. Curreli was a recipient of Marie Skłodowska-Curie Global Fellowship "2DTWIST." The fellowship is in collaboration with the Transport at Nanoscale Interfaces Laboratory, Swiss Federal Laboratories for Materials Science and Technology (EMPA), Switzerland. He was a recipient of the Young Scientists Award at the General Assembly and Scientific Symposium of URSI in 2022. He is also a member of the Topical Advisory Panel of Photonics and is an Academic Editor for the *Journal of Nanotechnology* and the *International Journal of Optics*. He is a part of the Committee of the Young Professionals Affinity Group of IEEE R8 Italy Section.



Matteo Bruno Lodi (Member, IEEE) received the bachelor's degree in biomedical engineering from the University of Cagliari, Cagliari, Italy, in 2016, the master's degree in biomedical engineering from Politecnico di Torino, Turin, Italy, in 2018, and the Ph.D.(Hons.) degree in electronic engineering and computer science from the University of Cagliari, Cagliari, Italy, in 2022.

From 2022 to June 2023, he was a Technologist with Electromagnetic Group, University of Cagliari, where he is currently an Assistant Professor. His research interests include the modeling of bioelectromagnetic phenomena, especially hyperthermia treatment, the study, manufacturing, and synthesis of magnetic biomaterials for tissue engineering applications, and the use of microwaves for biotechnology and environmental applications while working in the design and characterization of antennas for space and wearable applications.

Dr. Lodi was the recipient of the Young Scientists Award at the General Assembly and Scientific Symposium of URSI in 2020 and 2021, a Coauthor of the "2021 IEEE IST Best Student Paper Award" at the IEEE International Conference on Imaging Systems and Techniques, grant from the European Microwave Association for the attendance of the ESoA course titled "Diagnostic and Therapeutic Applications of Electromagnetics," and COST Action CA17115 for the attendance of the IX International School of Bioelectromagnetism Alessandro Chiabrera, where, in 2019, he was a recipient of the Best Poster Award. He is a member of the WG2: "Better thermal-based EM therapeutics" of the COST Action 17115 "MyWave." In 2022, he was appointed as the Chair of the IEEE Nanotechnology Council Young Professionals. He recently joined the NTC technical committee (TC2) Nanobiomedicine, in the frame of the MENE program. He is a member of the Editorial Board of the IEEE Future Directions Technology Policy and Ethics Newsletter.



Antonio Loddo received the bachelor's degree in technologies, viticultural, oenological, and food from the University of Sassari, Sassari, Italy, in 2019.

Since 2020, he has been working as a Researcher with Agency M.F.M. S.R.L. His research activity involves the food process engineering.



Giuseppe Mazzarella (Senior Member, IEEE) received the degree (*summa cum laude*) in electronic engineering from the Università Federico II of Naples, Naples, Italy, in 1984, and the Ph.D. degree in electronic engineering and computer science in 1989.

In 1990, he became an Assistant Professor with the Dipartimento di Ingegneria Elettronica, Università Federico II of Naples. Since 1992, he has been with the Dipartimento di Ingegneria Elettrica ed Elettronica, Università di Cagliari, Cagliari, Italy, first as an Associate Professor and then, since 2000, as a Full Professor, teaching courses in electromagnetics, microwave, antennas, and remote sensing. He is the author (or coauthor) of more than 100 articles in international journals and a reviewer for many EM journals. His research interests include the efficient design of large arrays of slots, power synthesis of array factor, with emphasis on the inclusion of constraints, microwave holography techniques for the diagnosis of large reflector antennas, use of evolutionary programming for the solution of inverse problems, in particular problems of synthesis of antennas and periodic structures.



Alessandro Fanti (Senior Member, IEEE) received the Laurea degree in electronic engineering and the Ph.D. degree in electronic engineering and computer science from the University of Cagliari, Cagliari, Italy, in 2006 and 2012, respectively.

From 2013 to 2016, he was a Postdoctoral Fellow with Electromagnetic Group, University of Cagliari, where he is currently an Assistant Professor. He has coauthored more than 100 scientific contributions published in international journals, conference proceedings, and book chapters. His research interests include the use of numerical techniques for modes computation of guiding structures, optimization techniques, analysis, and design of waveguide slot arrays, analysis, and design of patch antennas, radio propagation in urban environment, modeling of bioelectromagnetic phenomena, and microwave exposure systems for biotechnology and bioagriculture. He is a member of the IEEE Antennas and Propagation Society, the Italian Society of Electromagnetism, and the Interuniversity Center for the Interaction Between Electromagnetic Fields and Biosystems. From 2020 to 2023, he had been acting as a Principal Investigator of the IAPC Project, which was funded with five million euros by the Italian Ministry of Economic Development (MISE), within the AGRIFOOD PON I&C (2014–2020). Since 2024, he has been acting as a Principal Investigator of the AISAC Project, funded with 15 million euros by the Italian Ministry of Enterprises and Made in Italy (MIMIT), within the “ACCORDI PER L’INNOVAZIONE” (2021–2026). He is also an Associate Editor for the *IEEE Journal of Electromagnetics*, and *RF and Microwaves in Medicine and Biology*.

Open Access funding provided by ‘Università degli Studi di Cagliari’ within the CRUI CARE Agreement